Indian Journal of Engineering & Materials Sciences
Vol. 30, February 2023, pp. 103-111
DOI: 10.56042/ijems.v1i1.48945

Comparison of Signal Processing Techniques for Prediction of Optimal Process Variables to Yield Higher Productivity During Turning on CNC lathe

Pankaj Gupta[a], Bhagat Singh[b], & Yogesh Shrivastava[c]*

[a]Jaypee University of Engineering and Technology, Guna (M.P.), 473 226, India
[b]Galgotias College of Engineering and Technology, Greater Noida 201 310 , India

Received: 17 April 2021; Accepted: 21 September 2021

Tool chatter is one of such occurrences that limits MRR in a number of industries. In the current research, a method to boost output while lowering clatter during turning operations on a CNC lathe has been presented. A microphone is used to record the vibration signals generated during turning tests. The denoised signals are analysed using local mean decomposition (LMD). Disruptions and undesirable embedded ambient noise are removed using wavelet denoising (WD). The product functions that expose chatter information are chosen using these decomposed signals. To recreate the real-time chatter, these well-known PFs are used to reconstruct the signal. A consistent range of turning parameters for greater productivity has been created using the Grey relational analysis (GRA) prediction technique. The measured Chatter Index value has been found to denote steady turning, unstable, and moderate chatter circumstances. In order to confirm the validity of the presented methodology, several tests have been conducted.

Keywords: Chatter, Grey relational analysis, Local mean decomposition, Wavelet Denoising

1 Introduction

Chatter vibrations limit turning productivity and machining accuracy[1-4]. Once the chatter has been identified, suppressing it is a difficult undertaking[5,6]. According to some experts, the ideal cutting parameter settings can reduce noise. The SLD can be used to determine the ideal spindle speed and depth of cut[7]. Many researches ignore the important significance that feed rate has in choosing the cutting range. Reducing the feed rate and depth of cut, according to some researchers, helps lessen chatter[8,9]. SLD frequently lacks proper engineering assistance, making it impossible to estimate the ideal cutting range.

Consequently, a method that can identify the beginning of chatter is needed. The microphone is one of the sensors that is crucial in the capture of chatter signals. In order to collect audio signals during milling, researchers have employed microphones[10]. Additionally, it has been claimed that the captured chatter signals are distorted by background noise and obscure the genuine nature of the chatter features[11]. time-frequency domain analysis[12,13], as well as time-domain analysis[14]. The methods for detecting chatter that are most frequently employed are frequency domain analysis[15]. Huang[16] used cutting force variation to characterize the cutting stability. Through examination of prominent frequencies and energy ratios in the face milling operation, chatter identification has also been investigated using FFT spectrum[17]. These analyses' peak results are a result of chatter frequencies as well as unintentional contaminations and background noise. Therefore, it is crucial to get rid of these noise components before processing the signal to extract features[18].

During the milling of titanium super alloy, some researchers applied a chatter detection approach based on time series employing the recursive drawing method in combination with the Method Huang transform[12]. Wavelet packet decomposition, which served as a preprocessor to denoise the acquired signal, is how Cao[19] suggested measuring stability. Additional Hilbert-Huang transform (HHT) applications have improved HHT performance. For determining tool chatter features, several researchers have used HHT on empirical mode decomposition (EMD)[20]. They have demonstrated the efficiency of EMD in locating chatter bands, although it carries over the drawback of modal aliasing[21]. Additionally, when Hilbert transformation is applied to the findings of EMD decomposition, negative instantaneous frequency is more noticeable[22] which has largely been overcome by local mean decomposition[23], which also produces very good

*Corresponding author (Email: yogeshshrivastava90@gmail.com)

outcomes for identifying and examining chatter severity[24,25]. The decomposition findings of LMD are superior to those of EMD[26]. The LMD approach does, however, have some drawbacks. End effect and modal aliasing issues are not entirely resolved. The current research project was motivated by this.

Once chatter has been identified, the statistical parameter for the chatter index has been assessed for chatter feature extraction. Numerous studies demonstrate how cutting parameters affected the work material's surface quality[27]. In order to determine the impact of cutting parameters on turning operation, Chowdary *et al.*[28] investigated Taguchi. Using response surface approach, Abhang[29] examined surface roughness prediction (RSM). GRA has been used to investigate the mechanism of drilling and electrochemical discharge machining[30–32]. The previous researcher, however, did not use GRA to investigate the elements of chatter-free turning at a greater MRR. It was this that inspired the current study. Thus, in the current work, CI and MRR with regard to input parameters have been optimised using grey relational analysis (GRA).

In the present work single degree of freedom vibration system has been considered. The equation for (SDOF) forced vibration system is:

$$m\frac{d^2x(t)}{dt^2}+c\frac{dx(t)}{dt}+k\,x(t)=\Delta F(x,t) \quad \ldots (1)$$

Where, *m*=mass, *c*=damping coefficient and *k*=spring constant

It has been assumed for the purposes of this analysis that the workpiece's surface is smooth prior to cutting. After the initial rotation of the workpiece, the wavy surface is generated. The second revolution causes the generation of wavy surfaces on both the inside and outside of the cut (x(t) and x(t-T)), Consequently, for stability analysis is the equilibrium equation is;

$$\frac{d^2x(t)}{dt^2}+2\zeta\omega_n\frac{dx(t)}{dt}+\omega_n^2x(t)=\Delta\left(\frac{K_f}{m}a[h_0+x(t-T)-x(t)]\right) \quad \ldots (2)$$

Where, h_0=static thickness of chip, $h(t)$= ($x(t-T)-x(t)$)) is the dynamic thickness of chip, *T* is the time delay and a is the chip width.

The square and cubic terms[33] and power-law function for cutting force variation have both been taken into account to account for structural nonlinearities. Consequently;

$$\frac{d^2x(t)}{dt^2}+2\zeta\omega_n\frac{dx(t)}{dt}+\omega_n^2x(t)+\alpha_1x(t)^2+\alpha_2x(t)^3 =\Delta\left(\frac{K_f}{m}a[h_0+x(t-T)-x(t)]^{\frac{3}{4}}\right) \quad \ldots (3)$$

Apply third degree Taylor series; and considering,

$\beta_1=\frac{3}{4h_0}$, $\beta_2=-\frac{3}{32{h_0}^2}$, $\beta_3=\frac{5}{128{h_0}^3}$, x_T, Thus;

$=x(t-T)$, $x=x(t)$

$$\frac{d^2x}{dt^2}+2\zeta\omega_n\frac{dx}{dt}+\omega_n^2x+\alpha_1x^2+\alpha_2x^3 =-\frac{K_f}{m}ah_0^{\frac{3}{4}}\left[\beta_1(x-x_T)-\beta_1(x-x_T)^2+\beta_1(x-x_T)^3\right] \quad \ldots (4)$$

x has been expanded as third-order expansion.

$$x=\psi x_1(T_0,T_2)+\psi^2x_2(T_0,T_2)+\psi^3x_3(T_0,T_2)$$

Where, $T_0=t, T_2=\psi^2t$ *and* ψ *= small parameter of time scale* $\ldots (5)$

Depth of cut $a=a_c(1+\psi^2)$; and by substituting the value of a, x *and* $\frac{dx}{dt}, \frac{d^2x}{dt^2}$ from Equation (5) into Equation (4) and separating the same powers of function, the three delay differential equations are obtained;

$$\frac{\partial^2x_1}{\partial T_0^2}+2\zeta\omega_n\frac{\partial x_1}{\partial T_0}+\omega_n^2x_1+\beta_1\hat{K}(x_1-x_{1T})=0 \quad \ldots (6)$$

$$\frac{\partial^2x_2}{\partial T_0^2}+2\zeta\omega_n\frac{\partial x_2}{\partial T_0}+\omega_n^2x_2+\beta_1\hat{K}(x_2-x_{2T})=\beta_2\hat{K}(x_1-x_{1T})^2-\alpha_1x_1^2 \quad \ldots (7)$$

$$\frac{\partial^2x_3}{\partial T_0^2}+2\zeta\omega_n\frac{\partial x_3}{\partial T_0}+\omega_n^2x_3+\beta_1\hat{K}(x_3-x_{3T}) =-\frac{\partial^2x_1}{\partial T_2\partial T_0}-2\zeta\omega_n\frac{\partial x_1}{\partial T_2}+\hat{K}\begin{pmatrix}2\beta_2(x_1-x_{1T})\\(x_2-x_{2T})-\beta_3(x_1-x_{1T})^3\end{pmatrix} -\beta_1\hat{K}(x_1-x_{1T})-2\beta_1x_1x_2-\beta_2x_1^3 \quad \ldots (8)$$

Where, $\hat{K}=\frac{K}{m}a_ch_0^{\frac{3}{4}}$

By resolving the equations, it is possible to determine how nonlinear factors affect the stability

and amplitude response prediction of the system (6, 7 and 8). The analytical result is a complicated equation. The derived complex equation's real and fictitious parts are resolved. Finally, the chatter signal solution is stated as;

$$x(t)=\varepsilon w\cos(\omega_c t+\phi)$$

$$+\frac{1}{2}\varepsilon^2 w^2\left[\begin{array}{l}\frac{1}{M^2+N^2}\times\left(C_{1R}\cos 2(\omega_c t+\phi)\right)-\\ \left(C_{1I}\sin 2(\omega_c t+\phi)\right)+\frac{1}{\omega_n^2+\beta_1\hat{K}}\\ \left(2\beta_2\hat{K}(1-\cos\omega_c T)-\alpha_1\right)\end{array}\right] \quad \ldots (9)$$

Where,

$M=\omega_n^2-4\omega_c^2+\beta_1\hat{K}(1-\cos 2\omega_c T)$, $N=4\zeta\omega_n\omega_c+\beta_1\hat{K}\sin 2\omega_c T$

$C_{1R}=2\beta_2\hat{K}(1-\cos\omega_c T)\left(N\sin\omega_c T-M\cos\omega_c T\right)-\alpha_1 M$

$C_{1I}=2\beta_2\hat{K}(1-\cos\omega_c T)\left(N\cos\omega_c T+M\sin\omega_c T\right)+\alpha_1 N$

The chatter signal in turning operation has been simulated using equation (9). Additionally, Equation (9) is tampered with zero-mean white noise to mimic the actual working circumstances shown in Fig. 1.

2 Materials and Methods

2.1 Wavelet denoising technique (WDT)

The signal's noise makes it difficult to identify the chatter frequency precisely. The signal is denoised and undesired contaminations are eliminated using WDT. It can eliminate contaminants while preserving crucial information. The two following processes in this strategy are wavelet decomposition and thresholding. WDT stpes[34]: Apply a wavelet transform to a noisy signal to obtain noisy wavelet coefficients at a level that allows for adequate differentiation. Depending on the level and the threshold technique, choose the appropriate threshold limit. The thresholded wavelet coefficients are subjected to an inverse wavelet transform to produce a denoised signal. After passing the noisy signal through low- and high-pass filters, coefficients are then calculated. WDT involves condensing signal features into a small number of wavelet coefficients of large magnitude and denoising the small value coefficients by reducing or eliminating their values without compromising the true informative signal. Unwanted noise accounts for the lesser coefficients. In WDT, choosing the thresholding is a crucial step. There are two sorts of thresholding techniques: soft thresholding and harsh thresholding.

Soft thresholding;

$$W_{\lambda\_S}=\begin{cases}W_\lambda-\lambda & |W_\lambda|\geq\lambda\\ 0 & |W_\lambda|<\lambda\\ W_\lambda+\lambda & |W_\lambda|\leq-\lambda\end{cases} \quad \ldots (10)$$

Where, W_λ is the noisy wavelet coefficient and λ is the threshold. It is also called wavelet shrinkage, as values of coefficients shrinked towards zero.

Hard thresholding;

$$W_{\lambda\_H}=\begin{cases}W_\lambda & |W_\lambda|\geq\lambda\\ 0 & |W_\lambda|<\lambda\end{cases} \quad \ldots (11)$$

The hard thresholding either retains or discards coefficient values. Inverse wavelet transform produces the original signals that have been denoised after thresholding the coefficients.

2.2 Local mean decomposition (LMD)

Smith [23] published the LMD approach. In order to derive a time-varying instantaneous phase and instantaneous frequency, LMD deconstruct amplitude and frequency modulated signals into a limited number of product functions, each of which is the product of an envelope signal and a frequency modulated signal. A demodulated signal time-frequency representation can be created by plotting the instantaneous frequency and envelope values together.

2.3 Processing of the simulated signal with the suggested approach (WDLMD)

First, as shown in Fig. 2, Daubechies (db5) have been used along with two level decomposition to filter

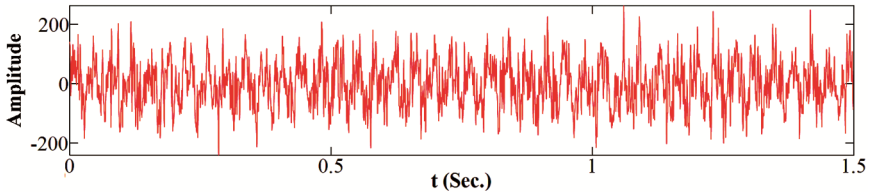

Fig. 1 — Simulated signal.

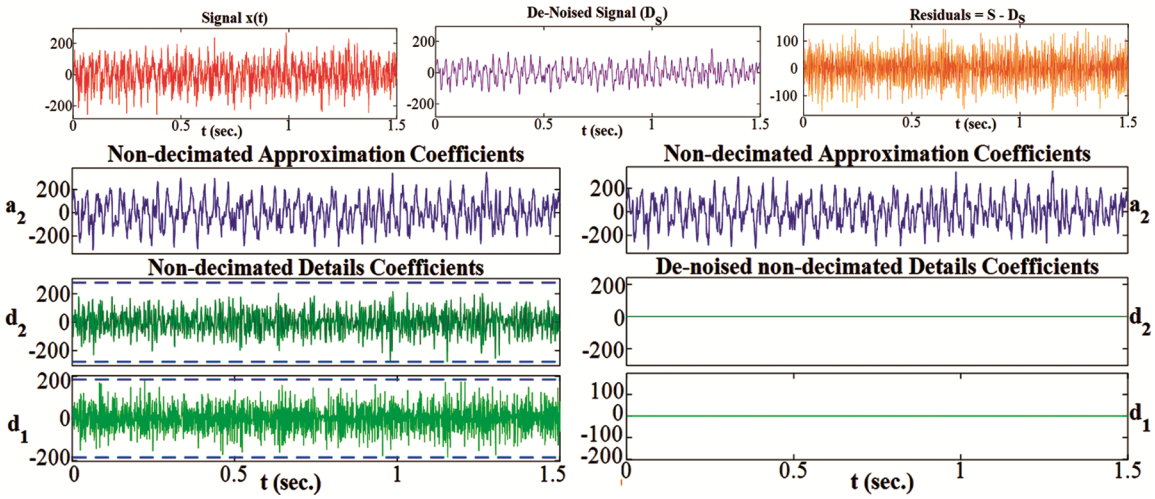

Fig. 2 — Wavelet denoising.

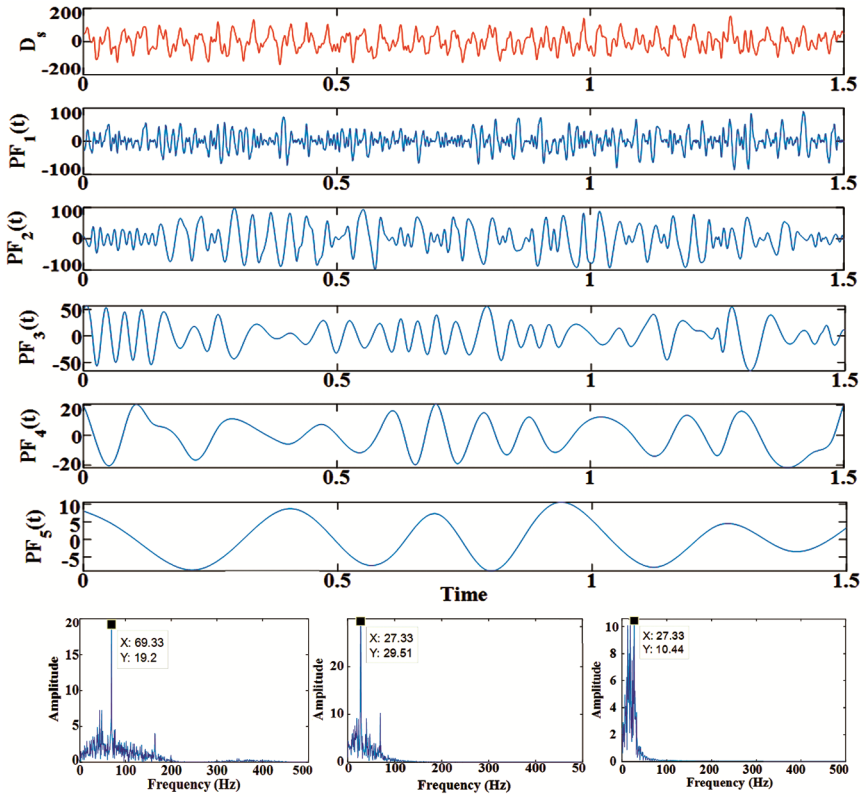

Fig. 3 — Product functions and FFTs of denoised signal.

noise. The stationary detailed coefficients "d1" and "d2" are obtained when a signal goes through a high-pass filter. The achieved value, "a2," denotes the approximate coefficient and the lower frequency.

The original signal components have also been restored using the LMD approach, as seen in Fig. 3. It is evident from the FFT of PFs that the mode aliasing issue has almost been resolved.

The correlation coefficient for PF1, PF2, and PF3 is 0.48, 0.69, 0.35, and insignificant for the other product functions. Thus, signal reconstruction is carried out utilizing the first three PFs. The reconstructed signal's correlation coefficient is 0.92. The frequency components of the signal without mode mixing are then depicted in Fig. 4's FFT of the reconstructed signal. Peak chatter frequencies can be

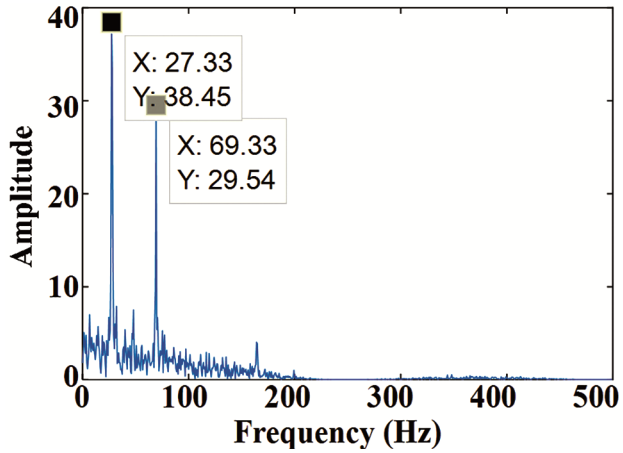

Fig. 4 — FFT of reconstructed signal.

readily seen in Fig. 4. As a result, the WDLMD approach may process the unprocessed chatter signals that contain noise.

2.4 Extracted features of real time turning experiment

The manufacturing sector's top priority in the current competitive environment is to produce goods of exceptional quality at a higher rate of output. In turning operations, productivity and material removal rate (MRR) are connected. Achieving a higher material removal rate can boost the productivity of certain manufacturing sectors. Additionally, the input process parameters of feed rate, spindle speed, and depth of cut all directly affect MRR. Higher these numbers, the greater the rate of material removal and, thus, the greater the productivity. By choosing a suitable range of machining parameters, MRR can be increased.

The surface quality of the end items is also influenced by these cutting factors. Therefore, it is crucial to consider how these machining parameters would affect surface finish when choosing them in order to get a greater MRR. Many vibrations are generated during the turning process when the tool and workpiece are in direct contact. These vibrations are referred to as self-excited vibrations or chatter vibrations. Chatter has an impact on machine tool assembly and production rate in addition to the quality of the final product. The researchers have demonstrated that the non-monotonic dependence of chatter severity on the aforementioned process factors. Therefore, it is important and pertinent to analyse chatter. Thus, in order to produce superior products at a higher material removal rate, a suitable range of machining parameters must be chosen.

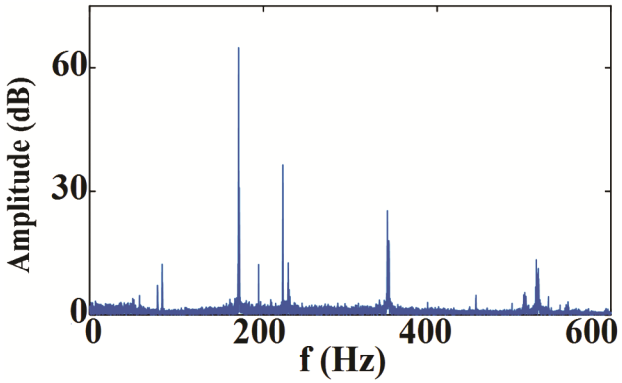

Fig. 5 — FFT of PFs and reconstructed signal.

Table 1 — Turning parameters

S. No.	Turning parameters	Level 1	Level 2	Level 3
1.	d (mm)	0.2	0.3	0.4
2.	n (rpm)	1000	1500	2000
3.	f (mm/min)	30	35	40

3 Results and Discussion

The studies were conducted using a CNC lathe equipped with MTAB XL-TURN after the suggested WDLMD approach was validated. Use is made of the cutting tool, workpiece Al-6061-T6, and carbide insert TTS04. The signal was recorded with an AHUJA AGN-480 dynamic unidirectional microphone with a sampling rate of 0.125 milliseconds. Additionally, data is acquired using MATLAB software, and a suggested signal processing technique is employed to determine the true nature of machining. According to Table 1, the experiments are carried out using a full factorial design.

3.1 WDLMD approach on acquired signals

Daubechies (db5) wavelet, 4 level decompositions have been used. Trial-and-error methods and decomposition that is compatible with the raw signal are used to choose the mother wavelet db5. The responsiveness of the chatter is improved by decomposition level 4. Each deconstructed level in this work has been subjected to soft thresholding. Standard deviation (σ) is to used to test thresholds. LMD was furthermore was used to demodulated signal. Correlation coefficient has been determined from the obtained PFs, and important PFs with built-in chatter information have been chosen. High correlation coefficient conspicuous PFs are used to build the reconstructed signal. As a result, it contains the most chatter frequency information. As seen in Fig. 5, the reconstructed signal of one experiment has distinct peaks in the FFT.

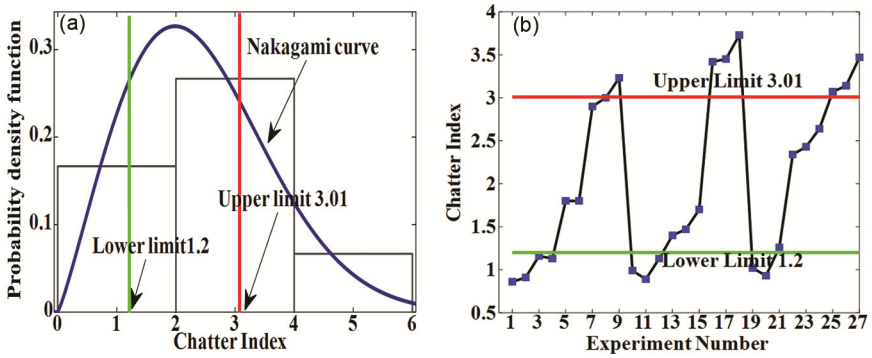

Fig. 6 — (a) PDF vs. CI, and (b) CI vs. Experiment number.

Table 2 — Turning parameters

S. No.	Turning parameters	Level 1	Level 2	Level 3
1.	d (mm)	0.2	0.3	0.4
2.	n (rpm)	1000	1500	2000
3.	f (mm/min)	30	35	40

3.2 Thresholding using Nakagami distribution

Chatter Index is calculated using the Equation (12), where $|x(t)|$ is signal and *N* sampling size;

$$Chatter\ Index\,(CI)=\frac{1}{N}\sum_{n=1}^{N}|x(t)| \quad \ldots (12)$$

According to Table 2, CI has been assessed for all 27 experiments. A lower CI value indicates a steady turn, while a greater number indicates an unstable turn. CI ranges in value from 0.86 at its lowest point to 3.73 at its highest. Following CI computation, a threshold has been established using the Nakagami distribution[35], as shown in Equation (13). Hence, PDF is calculated using shape parameter (μ) and spread parameter (□) as shown in Equation (13)

$$probability\ density\ function\,(PDF)$$
$$=\frac{2\mu^{\mu}}{\Gamma(\mu)\square^{\mu}}(CI)^{(2\mu-1)}e^{\left(-\frac{\mu}{\square}(CI)^2\right)} \quad \ldots (13)$$

Only when the shape parameter exceeds 0.5 and the spread parameter has a positive value for all positive random variables does this distribution fit the data. Using Matlab software, the PDF value and Nakagami curve are drawn. Fig. 6 displays probability density functions (PDF) and confidence intervals (CI) v/s experimental number. The spread parameter has a value of 5.16 while the shape parameter has a value of 1.23. It is clear from these measured values for the shape and spread parameters that the Nakagami distribution holds true in this instance of chatter analysis. Further, using $m \pm \sigma$ criterion, the upper and lower threshold limits are 3.01 and 1.2, respectively.

3.3 Metal removal rate (MRR)

$MRR=\frac{W_i-W_f}{t}$ Estimated *MRR* for all 27 experiments has been shown in Table 2.

3.4 Optimization process on variables for lower CI and higher MRR using GRA

Grey Relational Analysis (GRA)[32] was used in the current work primarily because it is one of the finest ways to determine the optimal value because it is based on original data, has simple calculations, and is uncomplicated. Using data from the Grey System, Grey Relational Analysis quantifies and dynamically compares the factors. It is utilized to establish the ideal relationship between different input parameters and output parameters in order to produce the best quality attributes. It is frequently used for assessing or appraising the effectiveness of a turning operation with scant information. The following are the GRA's steps:

Step 1: Data Pre Processing

This step normalizes the output parameters MRR and CI to a value between 0 and 1. The term "Grey relational generation" is another name for this normalization process. In this stage, GRA converted the original data's linear normalization

The following normalization applies to MRR, where greater is better and CI, where smaller is better:

Larger the better:

$$x_i(k)=\frac{\eta_i(k)-[\eta_i(k)]_{\min}}{[\eta_i(k)]_{\max}-[\eta_i(k)]_{\min}} \quad \ldots (14)$$

Smaller the better:

$$x_i(k)=\frac{[\eta_i(k)]_{\max}-\eta_i(k)}{[\eta_i(k)]_{\max}-[\eta_i(k)]_{\min}} \quad \ldots (15)$$

Table 3 — Chatter Index and MRR

Exp. No.	(d) mm	(n) rpm	(f) mm/min	Chatter Index (CI)	MMR (mg/sec)
1	0.2	1000	30	0.86	20
2	0.2	1000	35	0.91	23
3	0.2	1000	40	1.16	29
4	0.2	1500	30	1.13	20
5	0.2	1500	35	1.8	25
6	0.2	1500	40	1.8	29
7	0.2	2000	30	2.9	20
8	0.2	2000	35	3	25
9	0.2	2000	40	3.23	29
10	0.3	1000	30	0.99	30
11	0.3	1000	35	0.89	35
12	0.3	1000	40	1.13	40
13	0.3	1500	30	1.4	32
14	0.3	1500	35	1.47	38
15	0.3	1500	40	1.7	40
16	0.3	2000	30	3.42	32
17	0.3	2000	35	3.45	38
18	0.3	2000	40	3.73	43
19	0.4	1000	30	1.02	43
20	0.4	1000	35	0.93	48
21	0.4	1000	40	1.26	57
22	0.4	1500	30	2.34	40
23	0.4	1500	35	2.43	47
24	0.4	1500	40	2.64	48
25	0.4	2000	30	3.07	43
26	0.4	2000	35	3.14	56
27	0.4	2000	40	3.47	56

Equation 14 and 15 has been used to find out the normalized value of MRR and CI which is shown in Table 3.

Step 2: Grey relational coefficient (GRC) with Deviation sequence

The deviation sequence ($\Delta_{0i}(k)$) and GRC ($\gamma_i(k)$ values are;

$$\Delta_{0i}(k) = \left| x_0(k) - x_i(k) \right| \quad \ldots (16)$$

$$\gamma_i(k) = \frac{\Delta_{\min} + \zeta \Delta_{\max}}{\Delta_{0i}(k) + \zeta \Delta_{\max}} \quad \ldots (17)$$

GRC with deviation sequence for all 27 experiments has been presented in Table 4.

Step 3: Ranking with Grey relational grade (GRG)

The average total of the GRC values is identified as the GRG, and it is used to rank the studies. Equation 18 is employed in the calculation.

$$\gamma(x_0, x_i) = \frac{1}{2} \sum_{k=1}^{2} \gamma[x_0(k), x_i(k)] \quad \ldots (18)$$

Table 4 — Normalization of MRR and CI

Exp. No.	MMR (mg/sec)	Chatter Index (CI)	Normalized value (MMR)	Normalized value (CI)
1	20	0.86	0.000	1.000
2	23	0.91	0.081	0.983
3	29	1.16	0.243	0.895
4	20	1.13	0.000	0.906
5	25	1.8	0.135	0.672
6	29	1.8	0.243	0.672
7	20	2.9	0.000	0.289
8	25	3	0.135	0.254
9	29	3.23	0.243	0.174
10	30	0.99	0.270	0.955
11	35	0.89	0.405	0.990
12	40	1.13	0.541	0.906
13	32	1.4	0.324	0.812
14	38	1.47	0.486	0.787
15	40	1.7	0.541	0.707
16	32	3.42	0.324	0.108
17	38	3.45	0.486	0.098
18	43	3.73	0.622	0.000
19	43	1.02	0.622	0.944
20	48	0.93	0.757	0.976
21	57	1.26	1.000	0.861
22	40	2.34	0.541	0.484
23	47	2.43	0.730	0.453
24	48	2.64	0.757	0.380
25	43	3.07	0.622	0.230
26	56	3.14	0.973	0.206
27	56	3.47	0.973	0.091
Min	20	0.86	0	0
Max	57	3.73	1	1

The peak value of GRG is rank 1 and lowermost value of GRG is rank 27 in this work as shown in Table 5.

For each of the 27 sets of experiments, the calculated values of the GRG and the accompanying ranking for the various input turning parameters have been displayed. This table shows that the pairing with rank 1 produced the least amount of talk while improving MRR. Furthermore, the studies that produced the lowest rank, 27, had poor MRR values at higher chatter severity. Similar to this, the remaining experimental conditions may have been examined to understand the MRR and chatter severity. A primary effects plot has been created as shown in Fig. 7 in order to investigate the impact of input turning parameters on GRG. It is clear from this plot that the curve's slope (for cut depth) with respect to the horizontal axis is both positive and greatest. This shows that the depth of cut has a significant influence on both outputs. A modest increase in cut depth causes a significant rise in GRG. Therefore, for better performance, the depth of cut within the range under consideration should be lower. The inhomogeneity of the workpiece's material composition is what causes chatter. Due to the inhomogeneous nature

Table 5 — Deviation sequence and GRC

Exp. No.	Deviation sequence (MRR)	Deviation sequence (CI)	Grey relational coefficient (MRR)	Grey relational coefficient (CI)
1	1.000	0.000	0.333	1.000
2	0.919	0.017	0.352	0.966
3	0.757	0.105	0.398	0.827
4	1.000	0.094	0.333	0.842
5	0.865	0.328	0.366	0.604
6	0.757	0.328	0.398	0.604
7	1.000	0.711	0.333	0.413
8	0.865	0.746	0.366	0.401
9	0.757	0.826	0.398	0.377
10	0.730	0.045	0.407	0.917
11	0.595	0.010	0.457	0.980
12	0.459	0.094	0.521	0.842
13	0.676	0.188	0.425	0.727
14	0.514	0.213	0.493	0.702
15	0.459	0.293	0.521	0.631
16	0.676	0.892	0.425	0.359
17	0.514	0.902	0.493	0.357
18	0.378	1.000	0.569	0.333
19	0.378	0.056	0.569	0.900
20	0.243	0.024	0.673	0.953
21	0.000	0.139	1.000	0.782
22	0.459	0.516	0.521	0.492
23	0.270	0.547	0.649	0.478
24	0.243	0.620	0.673	0.446
25	0.378	0.770	0.569	0.394
26	0.027	0.794	0.949	0.386
27	0.027	0.909	0.949	0.355

Table 6 — GRG and Rank

Exp. No.	(d) mm	(n) rpm	(f) mm/min	GRG	Rank
1	0.2	1000	30	0.66667	7
2	0.2	1000	35	0.65936	9
3	0.2	1000	40	0.61247	11
4	0.2	1500	30	0.58749	13
5	0.2	1500	35	0.48527	20
6	0.2	1500	40	0.50103	19
7	0.2	2000	30	0.37314	27
8	0.2	2000	35	0.38387	26
9	0.2	2000	40	0.38749	25
10	0.3	1000	30	0.66176	8
11	0.3	1000	35	0.71816	4
12	0.3	1000	40	0.68138	5
13	0.3	1500	30	0.57593	15
14	0.3	1500	35	0.59752	12
15	0.3	1500	40	0.57595	14
16	0.3	2000	30	0.39224	24
17	0.3	2000	35	0.42493	23
18	0.3	2000	40	0.45128	22
19	0.4	1000	30	0.73446	3
20	0.4	1000	35	0.81311	2
21	0.4	1000	40	0.89101	1
22	0.4	1500	30	0.5067	18
23	0.4	1500	35	0.56333	16
24	0.4	1500	40	0.55954	17
25	0.4	2000	30	0.48146	21
26	0.4	2000	35	0.66749	6
27	0.4	2000	40	0.65174	10

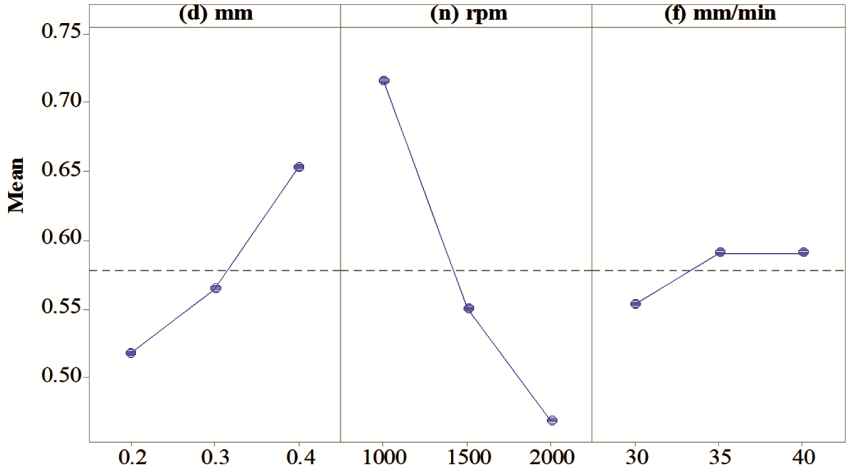

Fig. 7 — Main effects plot for GRG.

of the material, deeper cuts result non uneven tool penetration into the workpiece material.

For the subsequent turning passes, this generates scratched surfaces. The tool vibrates violently when it moves from one surface to another during these repeated turning passes, which is known as tool chatter in technical parlance. For rpm, a similar tendency has been noted. Additionally, the slope of feed rate is nearly parallel to the horizontal axis, indicating that feed rate's impact on GRG is not as significant. So, in order to obtain better performance, a moderate value of feed rate should be chosen.

As indicated in Table 6, the surface topographies of the machine surfaces have been rigorously studied to

validate the methodology for identifying the ideal process variable that corresponds to lower chatter and higher MRR. This table makes it clear that the suggested methodology is well suited for choosing the best process parameters for lower chatter and higher MRR when looking at the surface topographies, associated GRG, and rank. Additionally, the validity of this methodology is confirmed by comparing the MRR and CI values to the threshold limits determined by the Nakagami approach (Fig. 6).

4 Conclusion

The goal of this study is to find a consistent cutting range for CNC lathe turning operations that will produce a smooth surface finish at greater MRR. The key conclusions from this study are outlined as follows:

a The suggested WDLMD technique can extract the information from the chatter signal and remove the undesired noise items.

b FFT as spectrum analysis has been applied on reconstructed a signal that transforms the time domain signals into the frequency domain signals, which is assisting in the identification of the chatter frequencies.

c The chosen output parameter the CI exactly mimics chatter severity. Using CI it is easy to distinguish the severity of chatter during machining.

d Stability improves as spindle speed rises. However, when the cut gets deeper, dramatic chatter is seen. The feed rate has a moderate impact on chatter intensity.

e Nakagami distribution is important for determining the upper and lower bounds of different chatter domains.

f Grey relational analysis has capability to optimize the process variable in order to minimize one and maximize other, that help to figuring out the best set of process variables to use in order to get lower noise and increased productivity.

g Validation studies confirmed the value of a suggested GRA strategy for reaching the aforementioned goals.

References

1 Munoa J, Beudaert X, Dombovari Z,. Altintas Y, Budak E, Brecher C & Stepan G, *CIRP Ann Manuf Technol*, 65 (2016) 785

2 Mancisidor I,Pena-Sevillano A, Dombovari Z, Barcena R & Munoa J, *Mechatronics*, 63 (2019) 102276.

3 Wan M, Feng J, Ma Y C, Zhang W H, *Int J Mach Tools Manuf*, 122 (2017) 120.

4 Yang Y, Zhang W H, Ma Y C & Wan M, *Int J Mach Tools Manuf*, 109 (2016) 36

5 Tehranizadeh F, Berenji K R & Budak E, *Int J Mach Tools Manuf*, 171 (2021) 103813.

6 Gupta P & Singh B, *Appl Soft Comput*, 96 (2020) 106714.

7 Maamar A, Bouzgarrou B C, Gagnol V & Fathallah R, *Adv Acoust Vib*, (2017) 77

8 Siddhpura M, Siddhpura A & Paurobally R, *Int J Adv Manuf Technol*, 92 (2017) 881.

9 Gupta P & Singh B, *Acoust Aust*, (2020) 1.

10 Cao H, Yue Y, Chen X & Zhang X, *Int J Adv Manuf Technol*, 95 (2018) 961.

11 Shrivastava Y & B. Singh, *Eur J Mech A Solids*, 73 (2019) 381.

12 Rafal R, Pawel L, Krzysztof K, Bogdan K & Jerzy W, *Int J Mech Sci*, 99 (2015) 196.

13 Liu C, Zhu L & Ni C, *Int J Adv Manuf Technol*, 91 (2017) 3339.

14 Uekita M & Takaya Y, *Measurement,* 103 (2017) 199.

15 Fu Y, Zhang Y, Zhou H, Li D, Liu H, & Qiao H, *S. Mech Syst Signal Process*, 75 (2016) 668

16 Huang P, Li J, Sun J & Zhou J, *Int J Adv Manuf Technol*, 64 (2013) 613.

17 Wei C C, Liu M K, & Huang G H, *Int J Autom Smart Technol*, 6 (2016) 25.

18 Zhang Z, Li H, Meng G, Tu X & Cheng C, *Int J Autom Smart Technol*, 108 (2016) 106

19 Cao H, Lei Y & He Z, *Int. J Mach Tools Manuf*, 69 (2013) 11.

20 Shrivastava Y & Singh B, *Trans. Inst. Meas. Control,* 41 (2018).

21 Lian J, Liu Z, Wang H & Dong X, *Mech Syst Signal Process*, 107 (2018) 53.

22 Sandoval S, & Bredin, *Using Linear Prediction to Mitigate End Effects in Empirical Mode Decomposition*, paper presented at IEEE Global Conference on Signal and Information Processing GlobalSIP, 2018.

23 Gupta P & Singh B, *Appl. Soft Comput.*, 96 (2020) 106714.

24 Thameur K, Marc T, Raynald G & Mohamed E B, *Mech. Ind.*, 14 (2013) 121

25 Chen X & Yang Y, *De-noising for vibration signals based on local mean decomposition*, paper presented at IECON Annual Conference of the IEEE Industrial Electronics Society, IEEE, 2017.

26 Gupta P & Singh B, *J Vib Control,* (2020) 1077546320971157.

27 Gupta P & Singh B, *Exploration of tool chatter in CNC turning using a new ensemble approach*, paper presented at 1st International Conference on Energy, Material Sciences and Mechanical Engineering 2021.

28 Chowdary B V, Jahoor R, Ali F & Gokool F, *J Mech Eng*, 16 (2019) 77.

29 Azam M, Jahanzaib M, Wasim A & Hussain S, *Int J Adv Manuf*, 78 (2015) 1031.

30 Antil P, Singh S & Manna A, *Arab J Sci Eng*, 43 (2018) 1257.

31 Anand G, Alagumurthi N, Elansezhian R & Palanikumar K, *J. Braz Soc Mech,* 40 (2018) 1.

32 Mohammad H, Shahraki N, Taghiana S & Mirjalili S, *Expert Syst. Appl.*, 166 (2021) 113917.

33 Moradi H, Vossoughi G, Behzad M & Movahhedy M R, *Applied Mathematical Modelling*, 39 (2015) 600.

34 Bonda A, Nanda B & Jonnalagadda V, *Measurement*, 154 (2020) 107520.

35 Gupta P & Singh B, *Noise Vib Worldw*, 52(2021).